Materials and technologies for fabrication of three-dimensional microstructures with sub-100 nm feature sizes by two-photon polymerization

Frank Burmeister[a)]
Institute of Applied Physics, Friedrich-Schiller-Universität Jena, D-07743 Jena, Germany and Fraunhofer Institute for Applied Optics and Precision Engineering IOF, D-07745 Jena, Germany

Sönke Steenhusen[b)] and Ruth Houbertz
Fraunhofer Institute for Silicate Research ISC, D-97082 Würzburg, Germany

Uwe D. Zeitner, Stefan Nolte, and Andreas Tünnermann
Institute of Applied Physics, Friedrich-Schiller-Universität Jena, D-07743 Jena, Germany and Fraunhofer Institute for Applied Optics and Precision Engineering IOF, D-07745 Jena, Germany

(Received 14 October 2011; accepted for publication 10 June 2012; published 16 July 2012)

The fabrication of sub-100 nm feature sizes in large-scale three-dimensional (3D) geometries by two-photon polymerization requires a precise control of the polymeric reactions as well as of the intensity distribution of the ultrashort laser pulses. The authors, therefore, investigate the complex interplay of photoresist, processing parameters, and focusing optics. New types of inorganic–organic hybrid polymers are synthesized and characterized with respect to achievable structure sizes and their degree of crosslinking. For maintaining diffraction-limited focal conditions within the 3D processing region, a special hybrid optics is developed, where spatial and chromatic aberrations are compensated by a diffractive optical element. Feature sizes below 100 nm are demonstrated. © *2012 Laser Institute of America*.

Key words: two-photon polymerization, hybrid polymer, ORMOCER, refractive-diffractive hybrid optics, aberration correction

I. INTRODUCTION

In recent years, two-photon polymerization (2PP) has proven to be technology capable of fabricating arbitrary three-dimensional (3D) microstructures with feature sizes smaller than the diffraction limit of the applied laser wavelength.[1–4] Developments of new materials and illumination concepts like the STED lithography[5–7] have pushed the lateral dimensions of realizable structures below 100 nm. With the variability of the technology, several applications have emerged, e.g., in the field of micro-optics, where the fabrication of photonic crystals[8,9] or micro-optical elements[10–13] has been demonstrated. Furthermore, biomedical devices like scaffolds for cell growth[14–17] or small prostheses[18] could be realized.

Despite the ongoing progress in the field of 2PP, it remains challenging to preserve sub-100 nm feature sizes for complex three-dimensional microstructures with several 10 μm in height. This is mainly due to structuring depth dependent aberrations that occur when femtosecond laser pulses are focused with conventional microscope objectives into a nonindex-matched polymer. These aberrations lead to a decrease of the peak intensity in the focal plane and consequently to an inhomogeneous structuring process for different writing depths.

Besides the focusing optics and the applied process parameters, the molecular structure of the employed photopolymer plays an important role in structure formation as well as the achievable spatial resolution and surface roughness of the cured structures.

Therefore, we investigate the impact of material, process parameters, and focusing optics. Specially, adapted new types of the inorganic–organic hybrid polymer ORMOCER® were synthesized and characterized with respect to achievable feature sizes and degree of crosslinking (Sec. II). This gives a detailed insight into the impact of crosslinking chemical groups, photoinitiators, and laser parameters (pulse energy, exposure time) on structure formation. Furthermore, a refractive–diffractive hybrid optics for aberration-free focusing of the laser pulses into the polymer was developed and improvements for the volume structuring are presented (Sec. III).

II. MATERIAL SYNTHESIS AND PATTERNING

ORMOCER®s have become a material class of great interest for 2PP, since they combine favorable properties of glasslike materials, such as a high mechanical, thermal, and chemical stability with the ability to be photochemically patterned, which is well known from purely organic photoresists.[19–21] Furthermore, they exhibit excellent optical properties and biocompatibility, thus being a perfect material for micro-optical and biomedical applications.[22–26] For synthesis, alcoxysilane-precursors undergo hydrolysis and polycondensation reactions resulting in an organically modified inorganic-oxidic network ($[Si–O]_n$). This liquid resin can then be crosslinked photochemically and/or thermically resulting in solidified structures. As the reaction product

a)Electronic mail: Frank.Burmeister@iof.fraunhofer.de
b)Electronic mail: Soenke.Steenhusen@isc.fraunhofer.de

strongly depends on the choice of precursors and synthesis conditions, various properties of ORMOCER®s like stability, refractive index, and absorption behavior, as well as their molecular structure and polymerizable moiety can be tailored. Thus, there are several types of ORMOCER®s, each one adapted to one or more specific applications.

For efficient organic crosslinking of ORMOCER®s using 2PP suitable photoinitiators had to be identified, which show a high two-photon absorption cross-section, combined with a high quantum efficiency. Z-Scan experiments carried out on several commercial as well as specifically designed initiators revealed these conditions being met by some substances of the Ciba Irgacure® product line.[27,28] To investigate the resulting structure sizes for different material formulations and laser parameters, ascending scan experiments[29] were conducted on the methacrylic and acrylic ORMOCER®s OC-I and OC-V, respectively. In these studies, it turned out that in both ORMOCER® systems the achievable structure sizes did not reach the 100 nm threshold.[27]

One drawback of exploiting the material's threshold behavior in order to improve the spatial resolution is that the degree of polymer conversion, i.e., the degree of organic crosslinking, decreases dramatically when using lower photon fluxes. This affects the hardness of the solidified volume and, thus, the stability of 3D structures. A similar effect occurs when aberrations lead to a decrease of the peak intensity inside the volume of the polymer. The stability of voxels fabricated in the volume would diminish compared to voxels on the substrate. In order to quantify this loss of mechanical stability, we performed μ-Raman investigations on 2PP fabricated cube structures. These cubes were written in OC-I with different photon fluxes and hatching distances. We used a frequency-doubled Yb:YAG oscillator (t-Pulse 200, Amplitude Systemes) with a fundamental laser wavelength of 1030 nm, a pulse duration of 400 fs, and a repetition rate of 10 MHz in our experimental setup (described in detail in the literature).[4] To deduct the degree of polymer conversion, K, from the μ-Raman spectra, one needs a reference peak, which does not change upon illumination, and a peak of the crosslinking groups. In case of OC-I, the reference peak at 1570 cm^{-1} stems from ring vibrations of diphenylsilane-diol (DPD), whereas the C=C peak at 1640 cm^{-1} is an indicator for the organic crosslinking of the material. With the formula

$$K = 100 \times \left[1 - \frac{A_{1640}/A_{1570}}{A'_{1640}/A'_{1570}}\right],$$

K can be calculated,[24] where A denotes the area of the respective peaks of the polymerized structure and A' is the liquid ORMOCER® resin. Due to the overlapping of several peaks from initiator and ORMOCER® in the spectral region of interest, a deconvolution of peaks has been applied using the commercial software Omnic from Thermo Scientific. Two exemplary spectra of nonpolymerized and polymerized materials are shown in Fig. 1. As demanded, the peak at 1570 cm^{-1} is not affected after 2PP, whereas the peak at 1640 cm^{-1} diminishes. The results of our μ-Raman experiments are displayed in Fig. 2. As expected, the polymer conversion increases with increasing laser power until it reaches

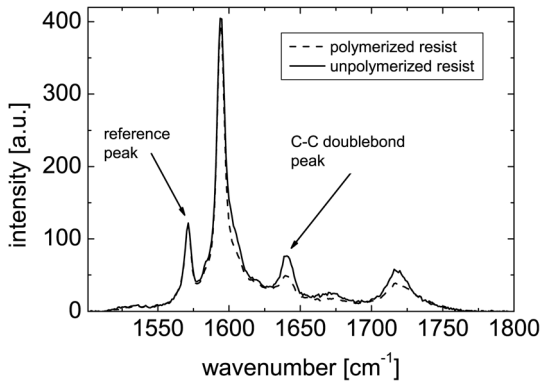

FIG. 1. μ-Raman spectra of unpolymerized OC-I (solid line) and polymerized structure (dashed line) fabricated by 2PP.

saturation at comparatively high laser powers. A further increase of power then does no longer affect the degree of crosslinking. The saturation value of approximately 80% is slightly higher compared to results found in thin layers of OC-I solidified using mask-aligner i-line illumination. Cubes with a K smaller than 35% were mechanically unstable and did not survive the solvent wash after illumination. This has to be kept in mind in the quest for 3D sub-100 nm 2PP lithography.

One aspect which is not yet entirely understood is the dependency of K on the hatching distance. The primary crosslinking of a single rod created during hatching of a cube should only be depending on the applied photon flux. But since we measured entirely polymerized cubes (rather than crystal structures with voids), single rods could not be measured. Actually, we average over overlapping rods, since their width is expected to be at least equal to or probably larger than the hatching distance. Furthermore, it has to be mentioned that even without the overlapping of rods, the measurement spot of the instrument always integrates over some rods, since its spatial resolution is, in contrast to 2PP, diffraction-limited. Therefore, the smaller distance of adjacent rods leads to measurement of higher conversion because of these two effects. This also agrees with the intuitive guess that structures with smaller hatching distances must be crosslinked stronger, because their total exposure time to laser pulses was longer, corresponding to higher exposure dose. Another issue might be the lifetime of radicals responsible for the crosslinking. Radicals created while writing a first rod might still influence the creation of the adjacent rod, if

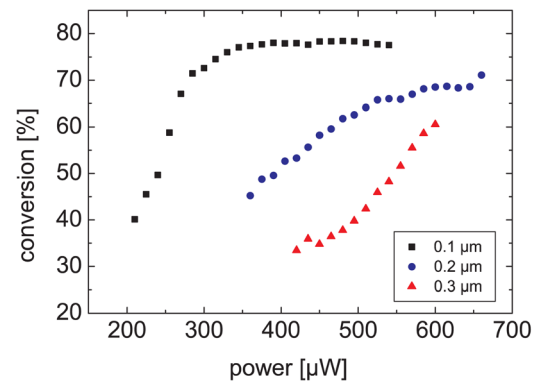

FIG. 2. Degree of C=C conversion in cubes fabricated from OC-I with different hatching distances and laser powers.

their lifetime is long enough and the adjacent rod is not too far away. This is subject of further investigations. In order to obtain a better understanding of crosslinking during the polymerization process, simulations of the molecular structure of the OC-I monomers and polymerization products are currently performed.[30]

Based on the findings from these preliminary experiments, a new ORMOCER® system, OC-II, was synthesized and patterned. In analogy to OC-I, it was synthesized from DPD and p-styryl-trimethoxysilane, i.e., the main difference is the polymerizable group, which is styryl in OC-II. Figure 3(a) depicts results of ascending scan experiments for average laser powers from 200 to 500 μW. Structure sizes below 100 nm can be achieved easily. In order to reveal the underlying scaling mechanism, Fig. 3(b) shows voxels of constant diameter plotted versus applied laser power and exposure time. We assumed an exposure dose $D \propto P^N t$ with P being the laser power and t the exposure time. A constant exposure dose D results in constant feature sizes. The dashed line corresponds to linear absorption ($N=1$) and the solid line to a two-photon absorption process ($N=2$). The good agreement of the slope of the solid line with the measured data indicates that two-photon absorption induced polymerization is the dominant process in structure formation. However, a possible contribution of thermal effects on the polymerization process caused by the high repetition rate of the laser system[31] has to be investigated in further experiments.

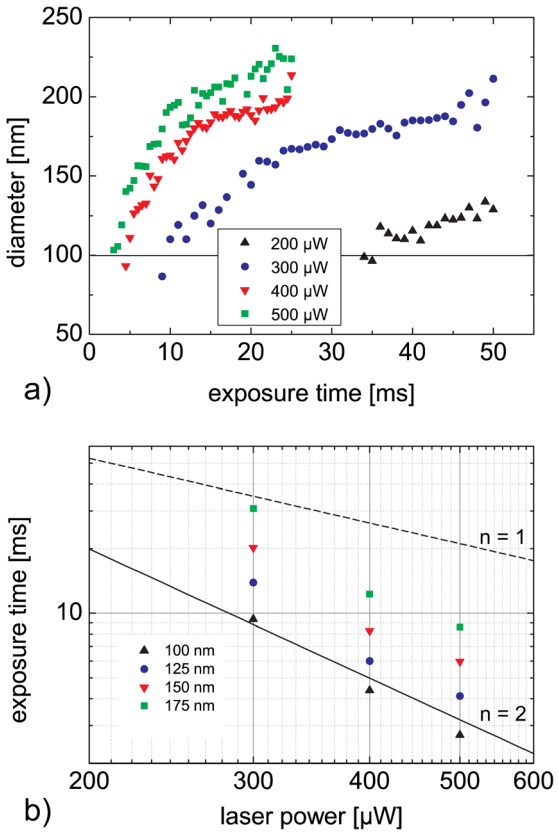

FIG. 3. (a) Results of ascending scans in OC-II with laser powers from 200 to 500 μW. (b) Logarithmic plot of points with constant diameter vs laser power and exposure time to reveal the scaling mechanism. The slope of the dashed line ($N=1$) corresponds to linear absorption, whereas the solid line ($N=2$) to a two-photon absorption process.

In Fig. 4, scanning electron microscope (SEM) images of some example structures are shown revealing 91 nm voxel sizes and line widths in the order of 100 nm. It is likely that the reactivity of the styryl group in comparison to the methacrylic group in OC-I leads to the improvement in feature size, although this has to be investigated in further detail as well.

III. OPTICAL DESIGN

In order to fabricate stable microstructures with a high degree of crosslinking and sub-100 nm feature sizes, aberration-free focusing of ultrashort laser pulses into the polymer for the complete structure height is needed. Usually, oil immersion microscope objectives with high numerical apertures (NAs) up to 1.45 are applied in setups for 2PP.[12,15] The laser pulses are focused through index-matching oil and a coverslip into the polymer located on the bottom of the coverslip. These conventional microscope objectives suffer from two main drawbacks when applied for 2PP. Diffraction-limited focusing of the laser pulses requires that the design conditions of the objectives are met, which are thickness and refractive index of the coverslip and usage of the proper immersion oil. Already a small change of the refractive index between coverslip and polymer leads to strong spherical aberration, whose amount mainly depend on the difference in the refractive indices, the focusing depth, and the NA of the objective.[32,33] Second, microscope objectives are complex optical systems consisting of several lenses causing a high group velocity dispersion (GVD), which leads to a temporal broadening of the laser pulses. In order to maintain the initial pulse duration, external compensation of the GVD is needed.

To overcome these drawbacks, we designed and manufactured a high numerical aperture hybrid optics specifically for the structuring of the ORMOCER® OC-I via 2PP. However, the optics can be easily adapted to other polymers (e.g., OC-II) as well.

The optics consists of merely three optical elements in order to keep the internal dispersion to a minimum: a diffractive optical element (DOE) for achromatization and the correction of spherical aberrations,[34] an asphere with NA = 0.6 (Edmund Optics 47 093), and a half ball lens working as a solid immersion lens (SIL) to increase the NA. The design of the hybrid optics allows for diffraction-limited focusing of the ultrashort pulses into the polymer with a numerical aperture NA = 1.33 over a working distance range of 550 μm. The optics is designed for focusing ultrashort pulses with a central wavelength of 515 nm and a spectral width of 3 nm

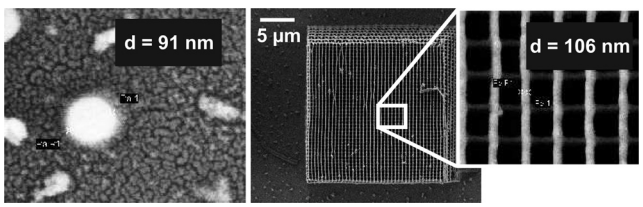

FIG. 4. SEM images of small features structured in OC-II. Left: Voxel fabricated with 164 μW and 100 ms. Right: Crystal like structure created with 550 μW and a feed rate of 50 μm/s.

[full width at half-maximum FWHM)]. Figure 5 shows the layout of the optics.

A SIL offers the possibility to significantly increase the NA of the asphere without introducing additional aberrations.[35–37] There are two possible configurations for the SIL. In the case of a hemispherical SIL, a hemisphere made of glass with refractive index n is placed with its center of curvature in the focus of the objective. When the rays enter perpendicular to the surface normal, no refraction occurs and the NA of the objective is increased by a factor n. Our design comprises an aplanatic solid immersion lens (ASIL). The ASIL consists of a hyper-hemisphere with radius R and refraction index n. For a center thickness of $d = R\left(1 + \frac{1}{n}\right)$, all geometrical aberrations from the ASIL are equal to zero.[38] The NA of the objective is increased by a factor n^2, due to the additional refraction at the surface of the ASIL.[39]

For three-dimensional structuring of the polymer, the ASIL has to be integrated into the setup in such a way that aberration-free focusing for variable focusing depths is possible. As shown in Fig. 5, the ASIL is composed of a half ball lens, immersion liquid, substrate and polymer. By choosing the polymer without the photoinitiator as immersion liquid, the total optical path inside the polymer remains constant for different focusing depths over the complete working distance. However, this setup introduces small spherical aberrations, since the ASIL no longer consists of one material with homogeneous refractive index. They can be minimized by choosing a glass for the half ball lens with a refractive index very close to that of the polymer. In our case, the half ball lens is made of N-SK11 with $n_d = 1.564$, almost exactly coinciding with $n_d = 1.563$ of the polymer.

For characterization, we compare our optics with an oil immersion microscope objective (Plan-Apochromat 100×, NA = 1.4, immersion oil Immersol $n_e = 1.518$, Zeiss) in terms of the structure sizes directly on the substrate surface as well as for different writing depths inside the polymer. In our experiments, a frequency-doubled Yb:YAG oscillator (t-Pulse 500, Amplitude Systemes) with a fundamental laser wavelength of 1030 nm, a pulse duration of 500 fs, and a repetition rate of 10 MHz is used. An acousto-optic modulator (AOM) is applied as shutter; the laser power is adjusted with a polarization beam splitter in combination with a half-wave plate.

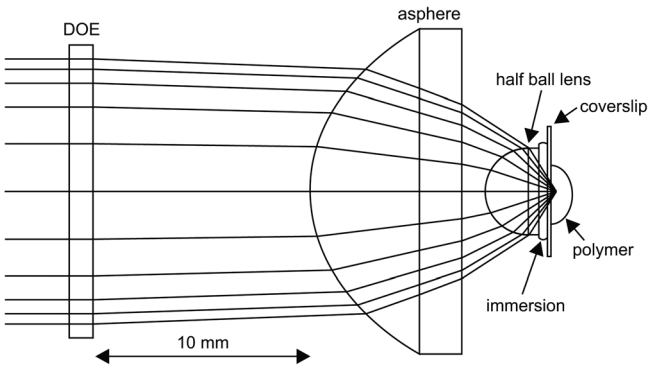

FIG. 5. Layout of the specifically designed hybrid optics consisting of an aspheric lens (Edmund Optics 47 093), a DOE, and a half ball lens (N-SK11, $r = 2$ mm) working as solid immersion lens.

For structuring directly on the substrate surface, the microscope objective as well as the hybrid optics are designed for diffraction-limited focusing. We applied point-by-point illumination of the polymer for different laser powers and exposure times to determine the smallest achievable size of the volume pixel (voxel). Figure 6 shows the resulting voxel sizes. For both objectives, the smallest achievable voxel diameters are slightly above 200 nm. The differences in the applied average powers (measured in front of the objectives) between Figs. 6(a) and 6(b) are due to the different aperture sizes of the objectives.

The improvements of the hybrid optics owing to the correction of writing depth dependent aberration become obvious, when applied for volume structuring of the polymer. We fabricated 30 μm high walls on the substrate that act as suspension for lines, written in different heights with constant writing parameters. The resulting line widths in dependence of the writing depth in the polymer can be seen in Fig. 7. The width of lines written with the Zeiss microscope objective [Fig. 7(a)] becomes smaller with increasing polymer thickness. This effect is caused by the spherical aberration that become stronger with increasing writing depth and the consequent drop of the peak intensity in the focal plane.[33] Apart from the changes in structure size, this drop

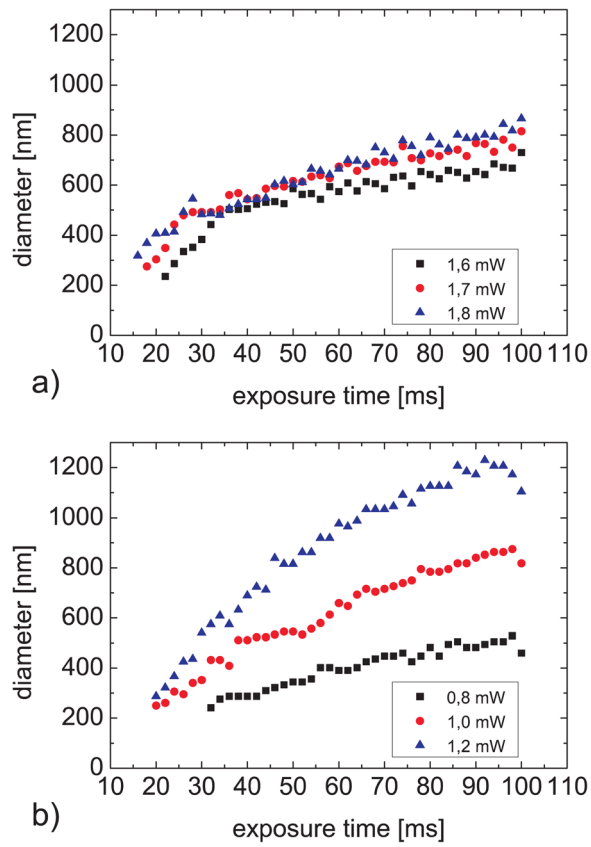

FIG. 6. Diameter of volume pixel on the substrate surface written with Zeiss Plan-Apochromat (a) and hybrid optics (b). In both cases, the smallest feature sizes are close to 200 nm. The differences in slope and separation between the curves in (a) and (b) are caused by the different aperture sizes of microscope objective and hybrid optics.

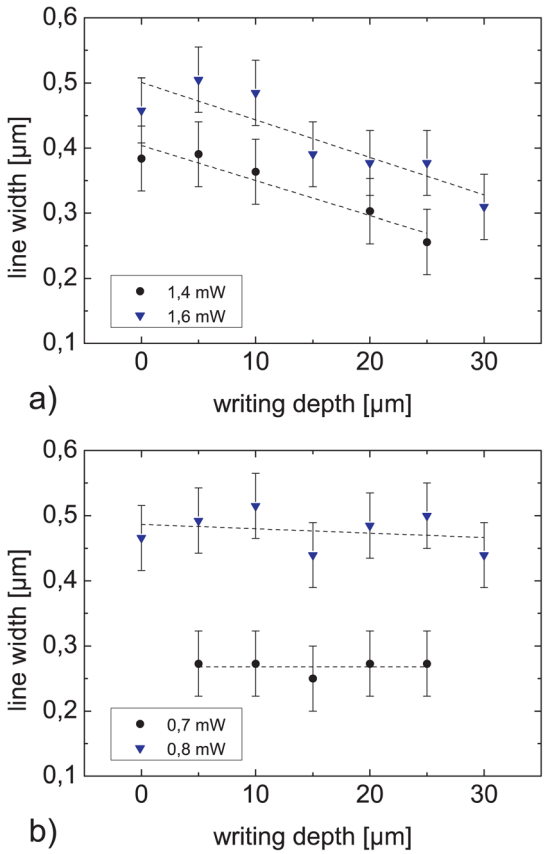

FIG. 7. Measured line width vs writing depth inside the polymer when focusing with the Zeiss Plan-Apochromat (a) and the hybrid optics (b). Scanning speed for all lines was 10 μm/s. Only (b) shows constant line widths for increasing writing depths and nonvarying writing parameters.

of the peak intensity also leads to a smaller degree of polymerization and, thus, to less stable structures (see Sec. II). In contrast, lines with steady widths for constant writing parameters in different writing depths can be fabricated, when the hybrid optics is applied for focusing into the polymer [Fig. 7(b)]. Due to the correction of the refractive index mismatch-induced spherical aberration, the hybrid optics should allow for homogeneous structuring with constant writing parameters over the complete working distance range of 550 μm (experimentally shown for 30 μm).

A further advantage of our optics is the low internal dispersion. The total GVD calculated from the dispersion curves of the optical materials used and the path lengths amounts to 842 fs^2, which is significantly less than the GVD of microscope objectives with comparable NA in the range of 2000 fs^2. Figure 8 shows the temporal broadening of the laser pulses in dependence of the initial pulse duration for hybrid optics and microscope objective. This indicates a significant difference for pulse durations shorter than 100 fs.

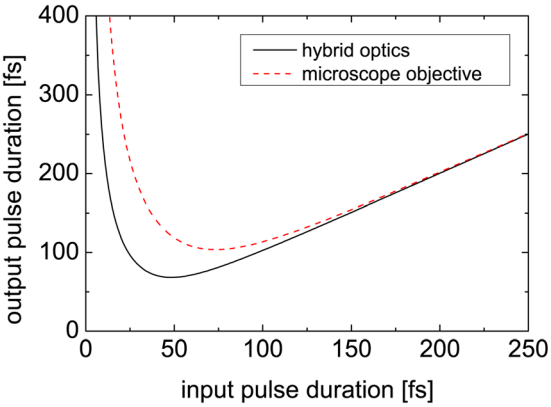

FIG. 8. Temporal broadening of laser pulses caused by the GVD of the focusing optics in dependence of the initial pulse duration. The values of the introduced GVD for hybrid optics and microscope objective are 842 fs^2 and 2000 fs^2, respectively.

IV. CONCLUSION

We investigated the influence of the polymer on structure size and presented a focusing concept that build the foundation for three-dimensional two-photon lithography of microstructures with features sizes on the sub-100 nm scale and high aspect-ratios. It could be shown that the newly synthesized ORMOCER® OC-II is suitable for the fabrication of nanostructures with dimension down to 91 nm. We realized a hybrid optics with a high numerical aperture NA = 1.33 for the aberration-free focusing of the laser pulses into the ORMOCER® OC-I. This optics allows for writing of microstructures with heights up to 550 μm without introducing index-mismatched induced aberrations. Owing to the reduced GVD of the hybrid optics, the temporal broadening of the focused laser pulses could be reduced compared to microscope objectives of comparable NA. The hybrid optics can be easily adapted to different polymers by changing the phase function of the DOE and choosing a material with a proper refractive index for the SIL.

The focusing concept in combination with the novel developed ORMOCER®s with their excellent optical properties and biocompatibility enables us to address future microoptical and biomedical applications.

ACKNOWLEDGMENT

The authors acknowledge financial support by the Deutsche Forschungsgemeinschaft (DFG) within priority Program No. SPP1327.

[1]S. Maruo, O. Nakamura, and S. Kawata, "Three-dimensional microfabrication with two-photon-absorbed photopolymerization," Opt. Lett. **22**, 132–134 (1997).
[2]B. H. Cumpston, S. P. Ananthavel, S. Barlow, D. L. Dyer, J. E. Ehrlich, L. L. Erskine, A. A. Heikal, S. M. Kuebler, I. Y. S. Lee, D. McCord-Maughon, J. Qin, H. Rockel, M. Rumi, X.-L. Wu, S. R. Marder, and J. W. Perry, "Two-photon polymerization initiators for three-dimensional optical data storage and microfabrication," Nature (London) **398**, 51–54 (1999).
[3]S. Kawata, H. B. Sun, T. Tanaka, and K. Takada, "Finer features for functional microdevices," Nature (London) **412**, 697–698 (2001).
[4]R. Houbertz, S. Steenhusen, T. Stichel, and G. Sextl, "Two-photon polymerization of inorganic-organic hybrid polymers as scalable technology using ultra-short laser pulses," in *Coherence and Ultrashort Pulse Laser Emission*, edited by F. J. Duarte (InTech, Rijeka, 2010).
[5]J. Fischer, G. von Freymann, and M. Wegener, "The materials challenge in diffraction-unlimited direct-laser-writing optical lithography," Adv. Mater. **22**, 3578–3582 (2010).
[6]J. Fischer and M. Wegener, "Three-dimensional direct laser writing inspired by stimulated-emission-depletion microscopy," Opt. Mater. Express **1**, 614–624 (2011).

[7]T. F. Scott, B. A. Kowalski, A. C. Sullivan, C. N. Bowman, and R. R. McLeod, "Two-color single-photon photoinitiation and photoinhibition for subdiffraction photolithography," Science **324**, 913–917 (2009).
[8]M. Deubel, G. von Freymann, M. Wegener, S. Pereira, K. Busch, and C. M. Soukoulis, "Direct laser writing of three-dimensional photonic-crystal templates for telecommunications," Nature Mater. **3**, 444–447 (2004).
[9]M. S. Rill, C. Plet, M. Thiel, I. Staude, G. von Freymann, S. Linden, and M. Wegener, "Photonic metamaterials by direct laser writing and silver chemical vapour deposition," Nature Mater. **7**, 543–546 (2008).
[10]S. Juodkazis, V. Mizeikis, and H. Misawa, "Three-dimensional microfabrication of materials by femtosecond lasers for photonics applications," J. Appl. Phys. **106**, 051101 (2009).
[11]E. Brasselet, M. Malinauskas, A. Zukauskas, and S. Juodkazis, "Photopolymerized microscopic vortex beam generators: Precise delivery of optical orbital angular momentum," Appl. Phys. Lett. **97**, 211108 (2010).
[12]M. Malinauskas, A. Zukauskas, V. Purlys, K. Belazaras, A. Momot, D. Paipulas, R. Gadonas, A. Piskarskas, H. Gilbergs, A. Gaidukeviciute, S. I. M. Farsari, and S. Juodkazis, "Femtosecond laser polymerization of hybrid/integrated micro-optical elements and their characterization," J. Opt. **12**, 124010 (2010).
[13]M. Malinauskas, H. Gilbergs, A. Zukauskas, V. Purlys, D. Paipulas, and R. Gadonas, "A femtosecond laser-induced two-photon photopolymerization technique for structuring microlenses," J. Opt. **12**, 035204 (2010).
[14]A. Doraiswamy, C. Jin, R. J. Narayan, P. Mageswaran, P. Mente, R. Modi, R. Auyeung, D. B. Chrisey, A. Ovsianikov, and B. Chichkov, "Two photon induced polymerization of organic-inorganic hybrid biomaterials for microstructured medical devices," Acta Biomater. **2**, 267–275 (2006).
[15]A. Ovsianikov, A. Ostendorf, and B. N. Chichkov, "Three-dimensional photofabrication with femtosecond lasers for applications in photonics and biomedicine," Appl. Surf. Sci. **253**, 6599–6602 (2007).
[16]S.-H. Lee, J. J. Moon, and J. L. West, "Three-dimensional micropatterning of bioactive hydrogels via two-photon laser scanning photolithography for guided 3D cell migration," Biomaterials **29**, 2962–2968 (2008).
[17]F. Klein, B. Richter, T. Striebel, C. M. Franz, G. Freymann, M. Wegener, and M. Bastmeyer, "Two-component polymer scaffolds for controlled three-dimensional cell culture," Adv. Mater. **23**, 1341–1345 (2011).
[18]A. Ovsianikov, B. Chichkov, O. Adunka, H. Pillsbury, A. Doraiswamy, and R. J. Narayan, "Rapid prototyping of ossicular replacement prostheses," Appl. Surf. Sci. **253**, 6603–6607 (2007).
[19]K. H. Haas, S. Amberg-Schwab, and K. Rose, "Functionalized coating materials based on inorganic-organic polymers," Thin Solid Films **351**, 198–203 (1999).
[20]U. Haas, A. Haase, V. Satzinger, H. Pichler, G. Leising, G. Jakopic, B. Stadlober, R. Houbertz, G. Domann, and A. Schmitt, "Hybrid polymers as tunable and directly-patternable gate dielectrics in organic thin-film transistors," Phys. Rev. B **73**, 235339 (2006).
[21]R. Infuehr, N. Pucher, C. Heller, H. Lichtenegger, R. Liska, V. Schmidt, L. Kuna, A. Haase, and J. Stampfl, "Functional polymers by two-photon 3D lithography," Appl. Surf. Sci. **254**, 836–840 (2007).
[22]R. Houbertz, P. Declerck, S. Passinger, A. Ovsianikov, J. Serbin, and B. N. Chichkov, "Investigations on the generation of photonic crystals using two-photon polymerization (2PP) of inorganic - organic hybrid polymers with ultra-short laser pulses," Phys. Status Solidi A **204**, 3662–3675 (2007).
[23]R. Houbertz, G. Domann, C. Cronauer, A. Schmitt, H. Martin, J. U. Park, L. Frohlich, R. Buestrich, M. Popall, U. Streppel, P. Dannberg, C. Wächter, and A. Bräuer, "Inorganic-organic hybrid materials for application in optical devices," Thin Solid Films **442**, 194–200 (2003).
[24]R. Houbertz, G. Domann, J. Schulz, B. Olsowski, L. Frohlich, and W. S. Kim, "Impact of photoinitiators on the photopolymerization and the optical properties of inorganic-organic hybrid polymers," Appl. Phys. Lett. **84**, 1105–1107 (2004).
[25]R. Houbertz, H. Wolter, V. Schmidt, L. Kuna, V. Satzinger, C. Wchter, and G. Langer, "Optical waveguides embedded in PCBs - a real world application of 3D structures written by TPA," Mater. Res. Soc. Symp. Proc. **1054**, 1054FF0104 (2007).
[26]A. Doraiswamy, T. Patz, R. J. Narayan, B. Chichkov, A. Ovsianikov, R. Houbertz, R. Modi, R. Auyeung, and D. B. Chrisey, "Biocompatibility of CAD/CAM ORMOCER polymer scaffold structures," Mater. Res. Soc. Symp. Proc. **845**, AA2.4 (2005).
[27]S. Steenhusen, T. Stichel, R. Houbertz, and G. Sextl, "Multi-photon polymerization of inorganic-organic hybrid polymers using visible or IR ultrafast laser pulses for optical or optoelectronic devices," Proc. SPIE **7591**, 759114 (2010).
[28]K. J. Schafer, J. M. Hales, M. Balu, K. D. Belfield, E. W. van Stryland, and D. J. Hagan, "Two-photon absorption cross-sections of common photoinitiators," J. Photochem. Photobiol., A **162**, 497–502 (2004).
[29]H. B. Sun, T. Tanaka, and S. Kawata, "Three-dimensional focal spots related to two-photon excitation," Appl. Phys. Lett. **80**, 3673–3675 (2002).
[30]S. Fessel, A. M. Schneider, S. Steenhusen, R. Houbertz, and P. Behrens, J. Sol-Gel Sci. Technol. (2012) published online.
[31]M. Malinauskas, P. Danilevicius, and S. Juodkazis, "Three-dimensional micro-/nano-structuring via direct write polymerization with picosecond laser pulses," Opt. Express **19**, 5602–5610 (2011).
[32]M. J. Booth and T. Wilson, "Refractive-index-mismatch induced aberrations in single-photon and two-photon microscopy and the use of aberration correction," J. Biomed. Opt. **6**, 266–272 (2001).
[33]M. J. Nasse and J. C. Woehl, "Realistic modeling of the illumination point spread function in confocal scanning optical microscopy," J. Opt. Soc. Am. A **27**, 295–302 (2010).
[34]U. Fuchs, U. D. Zeitner, and A. Tünnermann, "Hybrid optics for focusing ultrashort laser pulses," Opt. Lett. **31**, 1516–1518 (2006).
[35]S. M. Mansfield and G. S. Kino, "Solid immersion microscope," Appl. Phys. Lett. **57**, 2615–2616 (1990).
[36]I. Ichimura, S. Hayashi, and G. S. Kino, "High-density optical recording using a solid immersion lens," Appl. Opt. **36**, 4339–4348 (1997).
[37]S. B. Ippolito, B. B. Goldberg, and M. S. Ünlü, "High spatial resolution subsurface microscopy," Appl. Phys. Lett. **78**, 4071–4073 (2001).
[38]M. Lang, E. Aspnes, and T. D. Milster, "Geometrical analysis of third-order aberrations for a solid immersion lens," Opt. Express **16**, 20008–20028 (2008).
[39]S. B. Ippolito, B. B. Goldberg, and M. S. Ünlü, "Theoretical analysis of numerical aperture increasing lens microscopy," J. Appl. Phys. **97**, 053105 (2005).